S=1/2 magnetic chains as domain wall systems

1991 J. Phys.: Condens. Matter 3 2985

(http://iopscience.iop.org/0953-8984/3/17/015)

J. Phys.: Condens. Matter 3 (1991) 2985–3006. Printed in the UK

$S = \frac{1}{2}$ magnetic chains as domain wall systems

H J Mikeska, S Miyashita† and G H Ristow
Institut für Theoretische Physik, Universität Hannover, Federal Republic of Germany

Received 30 April 1990, in final form 21 December 1990

Abstract. We describe $S = \frac{1}{2}$ Ising-like magnetic chains completely in terms of domain walls. We formulate domain wall creation and annihilation operators as fermion operators and calculate the domain wall content of the ground state and of excited states. From exact results for finite chains and from the solution in the one-domain wall subspace we find that a single domain wall behaves like a free particle in a well. The transition between the two equivalent ground states of Ising-like $S = \frac{1}{2}$ chains is found to be dominated by quantum diffusion: the approach of the magnetization to the asymptotic behaviour is algebraic and not exponential. The analogy of this observation to interface fluctuations in the two-dimensional classical system is pointed out. For domain walls in the presence of impurities we study the phase shift and the transmission coefficient as well as the exact energy spectrum of finite impure lattices. To visualize the domain wall scattering we also demonstrate their real-time dynamics.

1. Introduction

In recent years domain wall- or soliton-like excitations have been theoretically recognized (Mikeska 1978, 1981) and experimentally verified (Kjems and Steiner 1978, Steiner *et al* 1983, Regnault *et al* 1983) as important elementary excitations in both ferromagnetic and antiferromagnetic chain systems. Both the dynamic, in particular the dynamic structure factor as measured in neutron scattering experiments, and the static (e.g. the specific heat) properties of these systems clearly show contributions from solitons as reviewed, among others, by Steiner and Bishop (1986) and Mikeska and Steiner (1990). Although the magnetic ions have rather low spin values in the magnetic model substances most widely used—$S = 1$ and $\frac{1}{2}$, respectively, in the ferromagnetic chain compounds $CsNiF_3$ and CHAB, $S = \frac{5}{2}$ in the antiferromagnetic compound TMMC—a classical description of solitons is used widely in agreement with the fact that the soliton is a classical concept.

Despite the fact that this classical description is surprisingly successful, it is interesting both from a fundamental as well as from a practical point of view to study the analogue of classical soliton excitations in genuine quantum systems. It is the purpose of the present paper to present such a study for spin chains with $S = \frac{1}{2}$, which on the one hand are genuine quantum systems of real experimental interest, and on the other hand in the Ising limit display the domain wall as basic excitation in direct analogy to the classical

† Permanent address: Department of Physics, College of Liberal Arts and Sciences, Kyoto University, Kyoto, 606 Japan.

0953-8984/91/172985 + 22 $03.50

case. We will thus deal with magnetic chains of Ising symmetry and will consider Hamiltonians of the following type

$$\mathcal{H} = -2J \sum_{n=1}^{N-1} S_n^x S_{n+1}^x + \mathcal{H}' = \mathcal{H}_{\text{Ising}} + \mathcal{H}'. \tag{1.1}$$

The first term in (1.1) is the Ising Hamiltonian (we will take the x direction as the direction of possible long range order throughout this paper) and the perturbing contribution $\mathcal{H}'$ is one of the following:

$$\mathcal{H}_1' = -2J\varepsilon \sum_{n=1}^{N-1} (S_n^y S_{n+1}^y + S_n^z S_{n+1}^z) \tag{1.2}$$

(Ising model with transverse interactions or xxz model),

$$\mathcal{H}_2' = -2J \frac{1-\gamma}{1+\gamma} \sum_{n=1}^{N-1} S_n^y S_{n+1}^y \tag{1.3}$$

(anisotropic xy model),

$$\mathcal{H}_3' = -H \sum_{n=1}^{N} S_n^z \tag{1.4}$$

(Ising model in a transverse field).

These systems are convenient for our purposes for two reasons:

(i) The classical analogues of these systems have been rather well investigated with respect to their soliton induced properties. Close to the Ising limit classical domain walls are extremely localized (for the model $\mathcal{H}_3'$ see e.g. Prelovšek and Sega 1981), whereas in the opposite limit the domain walls can approach those described by the classical sine–Gordon chain (as discussed by Elstner and Mikeska (1989) for the model described by $\mathcal{H}_2'$).

(ii) For spin $\frac{1}{2}$ the exact solution for the spin chain Hamiltonians given above is known generally from the Bethe *ansatz* approach; this solution is particularly simple for models $\mathcal{H}_2'$ and $\mathcal{H}_3'$, where the Hamiltonians can be explicitly diagonalized introducing fermion operators (Lieb *et al* 1961).

Since this solution is continuous in the interaction parameters, it is clear that the basic fermion excitation will be related to the domain wall of the Ising chain and we will exploit this relation in detail in section 2. We will introduce domain wall creation and annihilation operators and describe our chains completely in terms of domain walls mediating between the two degenerate ground states, which characterize the model chains above (for non-vanishing γ and $1-\varepsilon$ in the xy and xxz cases respectively), when infinitely long chains with free ends are considered (Lieb *et al* 1961, Pesch and Mikeska 1978). Close to the Ising limit the eigenstates are grouped in bands with a fixed number of domain walls.

In the usual treatment with periodic or free boundary conditions the immediate significance of domain walls is obscured by the translational invariance and by the twofold symmetry of the Ising like Hamiltonian. In the thermodynamic limit, the boundary conditions can be ignored for properties such as the specific heat, the nature of the system being determined by a characteristic length. Thus the individual domain wall has a fundamental role in thermodynamics (Mikeska and Steiner 1990). With

periodic boundary conditions, the spin-wave like excitations are the fundamental excitations (Ishimura and Shiba 1980), but they can be expressed by a combination of two domain walls in the thermodynamic limit. Normally, the effects of domain walls are therefore seen only indirectly. To display the spatial structure of domain walls more directly, we will consider different boundary conditions in section 2: by fixing the first and last spins in directions opposite to each other, we force the chain to have at least one domain wall which, then, can be investigated in real space and compared with its classical analogue. An approximate analytical approach to this question is given by restricting ourselves to the one-domain wall subspace; the quality of this approximation is checked by solving the same problem numerically for finite chains. The results from these two approaches completely agree. We find that the quantum domain wall is never localized, quantum diffusion completely masks the exponential approach to the asymptotic value in the classical case. Thus there does not exist a characteristic length in domain walls for $S = \frac{1}{2}$ Ising-like magnetic chains. The relation of this quantum delocalization of domain walls to the roughening problem is discussed in an appendix. In section 3 we will illustrate the domain wall description by considering the scattering of domain walls in magnetic chains with impurities.

The $S = \frac{1}{2}$ Ising chain with small transverse interactions (model 1 above) is of direct experimental relevance, since it represents rather well the magnetic chain compound $CsCoCl_3$. The soliton related properties of this substance have been investigated (see e.g. Yoshizawa *et al* 1981) and the relation between soliton and spin-wave excitations has been discussed in some detail (Buyers 1983, Smit *et al* 1989, Mikeska and Steiner 1990). Theoretically this model was first analysed by Villain (1975) and our approach to this system and the results given below should be considered as a further development and generalization of his approach.

Although the present paper does not give any specific predictions for experimental results, it attempts to make clear where to expect characteristic experimental signatures of domain walls in quantum spin chains and, in the case of impure chains, suggests to look for the confinement of domain walls in a substance like $CsCoCl_3$. We intend to supplement these remarks with more specific calculations in the future.

Considering the marked difference in the shape of the domain wall between the $S = \frac{1}{2}$ chains to be described in this work and in the classical limit it is of course natural to ask how the behaviour in the classical limit is obtained when the spin length S is varied between $S = \frac{1}{2}$ and $S = \infty$. There exist investigations in the semiclassical limit $1/S \ll 1$ (Mikeska *et al* 1989), which show an increase of the soliton width owing to quantum effects. On the other hand, the present approximate approach of considering the one-domain wall subspace only can be generalized to arbitrary values of S. These results together with supporting numerical calculations lead to a rather complete picture of the dependence of the domain wall structure and mobility on the spin value S as well as on the transition between the extreme quantum and the classical limits and are as yet unpublished (Mikeska and Miyashita 1990).

2. Domain wall creation and annihilation operators in $S = \frac{1}{2}$ Ising-like chains

In this section we will formulate the Ising-like $S = \frac{1}{2}$ magnetic chains as defined in (1.1–1.4) completely in terms of domain wall operators and relate spin expectation values to domain wall averages. For this purpose we make use of the representation of these

Hamiltonians in terms of fermion operators c_n, c_n^+, as introduced by Lieb *et al* (1961). We define the fermion operators

$$c_n = \exp\left(i\pi \sum_{m=1}^{n-1} a_m^+ a_m\right) a_n \tag{2.1}$$

and note their relation to the original spin operators

$$S_n^x = \tfrac{1}{2}(a_n^+ + a_n) \qquad S_n^y = (1/2i)(a_n^+ - a_n) \qquad S_n^z = c_n^+ c_n - \tfrac{1}{2}. \tag{2.2}$$

To obtain the domain wall representation we introduce

$$A_n = c_n^+ + c_n \qquad B_n = c_n^+ - c_n \tag{2.3}$$

as intermediate operators with the properties

$$\begin{aligned} &A_n^+ = A_n \qquad B_n^+ = -B_n \\ &\{A_m, A_n\} = -\{B_m, B_n\} = 2\delta_{mn} \qquad \{A_m, B_n\} = 0. \end{aligned} \tag{2.4}$$

Starting from these operators, we define as domain wall operators

$$D_n = \tfrac{1}{2}(A_{n+1} + B_n) \qquad D_n^+ = \tfrac{1}{2}(A_{n+1} - B_n) \tag{2.5}$$

with fermion commutation relations

$$\{D_m^+, D_n\} = \delta_{mn} \qquad \{D_m^+, D_n^+\} = \{D_m, D_n\} = 0. \tag{2.6}$$

The reason why we call D_n^+, D_n domain wall operators become apparent when we consider their effect on an arbitrary basis state $|\alpha_1, \alpha_2, \ldots \alpha_N\rangle$ for a chain with free ends (sites 1 to N) ($\alpha = +$ or $-$, quantization axis is the x axis). By direct calculation we obtain

$$\begin{aligned} &D_n^+ |\alpha_1, \alpha_2, \ldots \alpha_n, \alpha_{n+1} \ldots \alpha_N\rangle = \tfrac{1}{2}(\alpha_n + \alpha_{n+1})| - \alpha_1, -\alpha_2, \ldots -\alpha_n, \alpha_{n+1} \ldots \alpha_N\rangle \\ &D_n | -\alpha_1, -\alpha_2, \ldots -\alpha_n, \alpha_{n+1} \ldots \alpha_N\rangle = \tfrac{1}{2}(\alpha_n + \alpha_{n+1})|\alpha_1, \alpha_2, \ldots \alpha_n, \alpha_{n+1} \ldots \alpha_N\rangle. \end{aligned} \tag{2.7}$$

D_n^+ (D_n) thus changes the orientation of all spins on sites 1 to n and produces phase factors to create or annihilate a domain wall between sites n and $n + 1$, respectively. When the spins on adjacent sites are antiparallel, a ferromagnetic domain wall already exists and D_n^+ gives zero. Depending on the initial state, D_n^+ creates either a *soliton* (spin change from $-$ to $+$, when one proceeds along the chain) or an *antisoliton* (spin change from $+$ to $-$). The difference between these two possibilities is reflected in the phase of the resulting state. From (2.7) it is also clear that D_n^+ and D_n interchange their role when antiferromagnetic coupling is considered: application of D_n leads from antiparallel to parallel spins at sites n and $n + 1$ and thus creates an antiferromagnetic domain wall. Likewise $D_n^+ D_n$ is seen to be a projector to the subspace with different spin orientations at sites n and $n + 1$ and is thus the domain wall number operator.

A special role is played by the domain wall operators referring to sites at the boundaries: to make the mapping from the usual fermion representation to the domain

wall representation complete we have to give A_1 and B_N in terms of domain wall operators. To do so we define

$$D_0 = \tfrac{1}{2}(A_1 + B_N) \qquad D_0^+ = \tfrac{1}{2}(A_1 - B_N). \tag{2.8}$$

In terms of the domain wall operators the Ising Hamiltonian takes the simple form (we consider ferromagnetic coupling for definiteness)

$$\mathcal{H}_{\text{Ising}} = -\tfrac{1}{2}J(N-1) + J\sum_{n=1}^{N-1} D_n^+ D_n. \tag{2.9}$$

The energy is thus obtained by counting the number of domain walls. D_0 and D_0^+ commute with $\mathcal{H}_{\text{Ising}}$; these operators are not domain wall operators, but serve instead to distinguish the two degenerate states resulting from turning around all spins. They transform between these states in the following way:

$$\begin{aligned}(D_0^+ + D_0)|\alpha_1, \ldots \alpha_N\rangle &= \alpha_1|\alpha_1, \ldots \alpha_N\rangle \\ (D_0^+ - D_0)|\alpha_1, \ldots \alpha_N\rangle &= \alpha_N|-\alpha_1, \ldots -\alpha_N\rangle.\end{aligned} \tag{2.10}$$

Spin chain Hamiltonians are now easily written in the domain wall representation as $\mathcal{H} = \mathcal{H}_{\text{Ising}} + \mathcal{H}'$, and we obtain in the three cases discussed above:

(i) *xxz* model:

$$\mathcal{H}_1' = -J\varepsilon\sum_{n=1}^{N-1}(-D_{n-1}^+ D_{n+1} + D_{n-1}^+ D_{n+1}^+ + \text{HC})D_n^+ D_n \tag{2.11}$$

(ii) anisotropic *xy* model:

$$\mathcal{H}_2' = J\frac{1-\gamma}{4(1+\gamma)}\sum_{n=1}^{N-1}(D_{n-1}^+ D_{n+1} - D_{n-1}^+ D_{n+1}^+ + \text{HC}) \tag{2.12}$$

(iii) Ising model in a transverse field:

$$\mathcal{H}_3' = -\tfrac{1}{2}H\sum_{n=1}^{N}(D_{n-1}^+ D_n - D_{n-1}^+ D_n^+ + \text{HC}). \tag{2.13}$$

Here we define $D_N := D_0$. As is well known for these fermion representations, the *xxz* model contains interactions between domain walls, whereas the remaining two models are free fermion models (involving both scattering and pair production and annihilation of domain walls, respectively), which can be diagonalized exactly.

Equations (2.9, 2.11–2.13) are remarkable since they provide a formulation of soliton supporting magnetic chains directly in terms of soliton creation and annihilation operators, whereas, so far, soliton theories have restricted themselves to one sector with a definite number of solitons from the beginning. An attempt to present a formulation in this spirit has actually been performed by Devreux and Boucher (1987); this, however, did not succeed in establishing a valid transformation from spin operators to fermions describing domain walls. Our formulation, on the other hand, only serves to show more

directly the problems involved in a direct creation of solitons by external fields. Let us consider the following relations between spin operators and domain wall operators

$$S_n^x = \tfrac{1}{2}(D_0^+ + D_0)\prod_{p=1}^{n-1}(1 - 2D_p^+ D_p) \tag{2.14}$$

$$S_n^y = (1/2\mathrm{i})(D_0^+ + D_0)\prod_{p=1}^{n-2}(1 - 2D_p^+ D_p)(D_{n-1}^+ D_n^+ - D_{n-1}^+ D_n - \mathrm{hc}) \tag{2.15}$$

$$S_n^z = \tfrac{1}{2}(D_{n-1}^+ D_n^+ - D_{n-1}^+ D_n + \mathrm{hc}). \tag{2.16}$$

All spin operators are bilinear in the operators D_n, D_n^+; the only way to change the number of domain walls by one using a single-spin operator is to consider boundary spins, since D_0 is not a domain wall operator as noted above. We have e.g.

$$S_1^y = (\mathrm{i}/2)(D_1^+ - D_1) \tag{2.17}$$

and similarly for S_1^z, S_N^y, S_N^z. Thus single domain walls are always created at the end of an open chain—this is exactly the same situation as one finds e.g. in the description of the generation of solitons in classical chains described by the sine-Gordon model. On the other hand, expressing the operator D_m^+ for arbitrary site m by spin operators gives

$$D_m^+ = \prod_{p=1}^{m}(2S_p^z)(S_m^x + S_{m+1}^x). \tag{2.18}$$

This transformation is highly non-linear and the required combination of spin operators to create a single wall is clearly not experimentally accessible.

In the following we will consider in some more detail the application of the domain wall representation to the Ising chain in a transverse field (model (iii) above). The Hamiltonian in the form of equations (2.9, 2.13) is easily diagonalized following the procedure of Lieb *et al* (1961); the result for the open chain with $H < J$ (which is the case of a non-trivial groundstate) is

$$\mathcal{H} = -\tfrac{1}{2}J(N-1) + \sum_{p=1}^{N-1}\Lambda_{q_p}\eta_{q_p}^+\eta_{q_p} + \Lambda_0\eta_0^+\eta_0 \tag{2.19}$$

with

$$\eta_q^+ = \sum_n (g_{qn}D_n^+ + h_{qn}D_n) \qquad g_{qn} = \tfrac{1}{2}(\Phi_{qn} + \Psi_{qn}) \qquad h_{qn} = \tfrac{1}{2}(\Phi_{qn} - \Psi_{qn}) \tag{2.20}$$

$$\Lambda_q = \sqrt{1 + h^2 + 2h\cos(q)} \qquad h = H/J. \tag{2.21}$$

The $N-1$ real q values and one complex solution $q = q_0 = \pi + \mathrm{i}\kappa$ (which we denote by the index 0), are determined from the equation

$$\sin(qN) + h\sin[q(N+1)] = 0. \tag{2.22}$$

The $N-1$ real q values are of the form $q_p = (p - \varepsilon_p)\pi/N$, $0 < \varepsilon_p < 1$, $p = 1, \ldots N-1$, and the eigenvectors (we define $\Psi_{q0} \equiv \Psi_{qN}$) are given by:

real solutions,

$$\Phi_{q_p n} = N_q(-1)^p \sin[q(n-N)]$$
$$\Psi_{q_p n} = N_q \sin(qn) \tag{2.23}$$
$$N_q^{-2} = N/2 - \cos[q(N+1)] \sin(qN)/2\sin(q)$$

complex solution,

$$\Phi_{0n} = N_0(-1)^n \sinh[\kappa(n-N)]$$
$$\Psi_{0n} = N_0 \sinh(\kappa n) \tag{2.24}$$
$$N_0^{-2} = -N/2 + \cosh[\kappa(N+1)] \sinh(\kappa N)/2\sinh(\kappa).$$

For $N \to \infty$ one has $\Lambda_0 \sim h^N \to 0$, i.e. the ground state is twofold degenerate. These results, of course, are nothing but a variant of the treatment of the Ising model in a transverse field in the fermion representation (Pfeuty 1970). In the present context we want to use these results to discuss the properties, which characterize the domain wall aspects of this model. For this purpose we have calculated expectation values for the following states, which evolve continuously to the degenerate domain wall states of the Ising model for $h \to 0$:

$$|0\uparrow\rangle = (1/\sqrt{2})(1 - \eta_0^+)|0\rangle \tag{2.25}$$
$$|m\rangle = D_m^+|0\uparrow\rangle \tag{2.26}$$

Here $|0\rangle$ is one of the two degenerate ground states, i.e. in the fermion language, $\eta_q|0\rangle = \eta_0|0\rangle = 0$. The state $|0\uparrow\rangle$ for $h \to 0$ evolves to the ordered groundstate of the Ising model with all spins up, whereas the state $|m\rangle$ is continuously related to the one-domain wall state of the Ising chain with a spin flip between sites m and $m+1$. The state $|m\rangle$ is constructed in similar manner as the state $|\Psi_m\rangle$ of Prelovšek and Sega (1981); however, the correlations induced by the transverse field are taken into account properly. We emphasize that $|0\uparrow\rangle$ is an eigenstate of the Hamiltonian for $N \to \infty$, whereas $|m\rangle$ should be considered as a wavepacket of eigenstates approximating an Ising domain wall as closely as possible.

Using these states we have calculated the following domain wall related properties:

(i) The domain wall content of the Ising-like groundstate:

$$\delta_n^{(0)} = \langle 0\uparrow|D_n^+ D_n|0\uparrow\rangle. \tag{2.27}$$

The result of the calculation for $N = 100$ is given in figure 1 for $n = 50$, i.e. a spin at the chain centre, and for $n = 1$, a boundary spin. One sees that, generally, the number of domain walls in the groundstate of the correlated chain grows rather slowly with h. Owing to the free boundary conditions the probability of the occurrence of a domain wall is somewhat larger for a spin close to the boundary than for a spin at the centre.

(ii) The domain wall content of the state $|m\rangle$:

$$\delta_n^{(m)} = \langle m|D_n^+ D_n|m\rangle. \tag{2.28}$$

Results are shown in figure 2. One sees that the domain wall density is strongly centred at the site $m = n$, which qualitatively confirms the physical motivation for the construction of the state $|m\rangle$. This is clearly visible for small values of h, see figure 2(a), whereas for finite values of h, see figure 2(b), a finite domain wall density (of the same

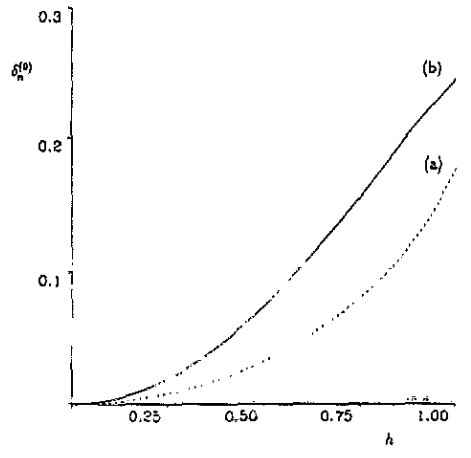

Figure 1. The domain wall content $\delta_n^{(0)}$ of the ground state of the Ising chain with $N = 100$ in a transverse field $H = hJ$ for (a) $n = 50$ and (b) $n = 1$.

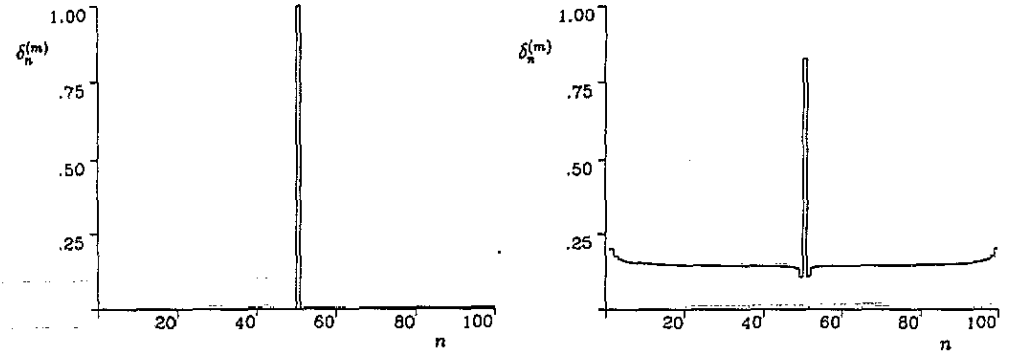

Figure 2. The domain wall content $\delta_n^{(m)}$ of the domain wall state $|m\rangle$ of the Ising chain with $N = 100$ in a transverse field for $n = 50$. (a) $H/J = 0.1$, (b) $H/J = 0.99$.

order of magnitude as in the groundstate) appears for sites $m \neq n$. This clearly reflects the fact that $|m\rangle$ is not an eigenstate of the Hamiltonian. As we will see below, it is not possible to construct localized domain wall states as eigenstates.

(iii) The spatial variation of the x component of spin, which characterizes the transition between the two degenerate ground states in real space and permits a direct comparison to the classical behaviour. In view of the highly non-linear relation between the spin operators and the domain wall operators, see (2.14) above, we have restricted ourselves in this case to the low density limit, using the approximation

$$\prod_{p=1}^{n-1} (1 - 2D_p^+ D_p) \approx 1 - \sum_{p=1}^{n-1} 2D_p^+ D_p. \tag{2.29}$$

From figure 3 it is clear that the general behaviour of $\langle S_n^x \rangle$ is as expected, showing the localized transition between the asymptotic values $\langle S_n^x \rangle = \pm 1$. The approximation (2.29), however, introduces numerical errors which accumulate with increasing n; meaningful results can therefore only be given for sufficiently small values of H/J. Of particular

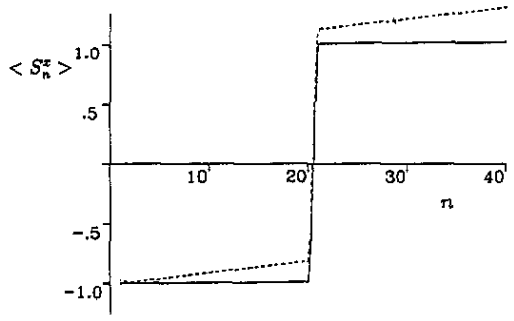

Figure 3. Spatial variation of $\langle S_n^x \rangle$ in a one-domain wall state $|m\rangle$ of the Ising chain in a transverse field ($N = 80$, $m = 20$) using (2.29). Full lines $H/J = 0.05$, broken lines $H/J = 0.2$.

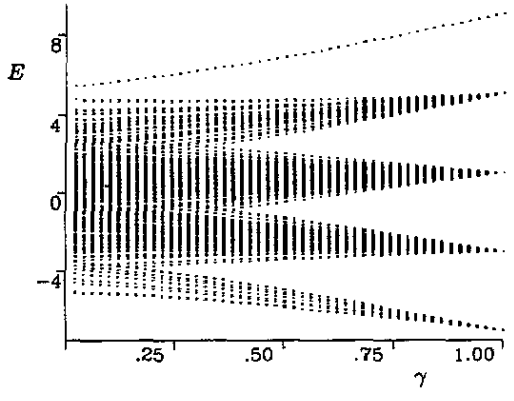

Figure 4. Dependence of the complete energy spectrum of the anisotropic xy chain with $N = 8$ on the anisotropy parameter γ.

interest is the approach to the asymptotic behaviour far from the centre of the wall. The analysis below shows that this approach is not exponential but governed by a power law.

The description of the quantum spin chain in terms of domain walls becomes particularly simple close to the Ising limit. Let us consider the anisotropic xy chain, (1.3), with strong magnetic fields $\pm B_b$ at the right (left) boundary of our chain to break the $\pm x$ symmetry and to force the chain to contain at least one domain wall. The resulting energy spectrum for a finite chain and in the limit $B_b \to \infty$ (tantamount to fixing the spins at the boundary sites as down and up, respectively) is given in figure 4 and shows, for $\gamma \ll 1$, states grouped in bands with 1, 3, 5 . . . domain walls. The energy difference between these bands is J, whereas the width of the bands for $\gamma \to 1$ is $J(1 - \gamma)$. We see that the splitting into distinct bands is the basic qualitative feature of the system for values of $\gamma \geqslant 0.5$. It thus appears to be a reasonable approximation in this parameter range to take into account only the lowest band, i.e. to restrict calculations to the one-domain wall subspace. Considering (2.11–2.13) this approximation amounts to neglecting the pair creation and annihilation terms and is equivalent to describing the domain wall as a free particle moving in a well; the condition of fixing the boundary spins by the symmetry breaking magnetic fields then translates into a vanishing of the wavefunction of this particle at the chain boundaries.

In order to both illustrate the one-domain wall approximation and to check its validity, we now consider the expectation value of the order parameter $\langle S_n^x \rangle$ for the

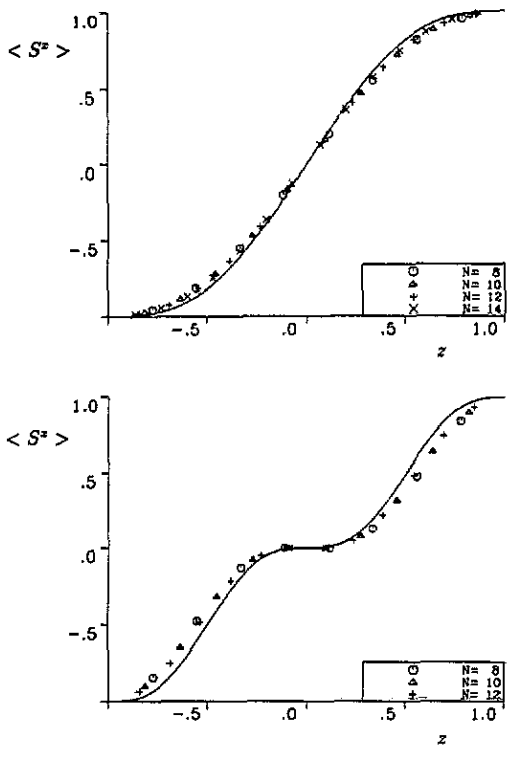

Figure 5. Spatial variation of $\langle S^x \rangle$ in a spin chain with boundary spins fixed at ± 1 to enforce the presence of a domain wall. Results of the one-domain wall approximation (full curves) are compared with finite chain results (see inset). (*a*) Ground state of the transverse field Ising model with $H/J = 0.1$. (*b*) First excited state of the transverse field Ising model with $H/J = 0.1$.

standard situation of a domain wall mediating between two equivalent groundstates to the far right and far left of its position respectively. We use a continuum description with spatial coordinate $z = 2n/N - 1$, $-1 \leqslant z \leqslant 1$. In the xxz chain with antiferromagnetic coupling and the anisotropic xy chain, this continuum approximation involves only either even or odd sites owing to the hopping by two sites, see (2.11, 2.12); apart from this difference all models become equivalent. The probability of the domain wall in the groundstate of the chain with fixed boundary spins $|\Psi_g\rangle$ being found at position z is then given by $|\Psi_g(z)|^2 = \cos^2[(\pi/2)z]$, which leads to

$$\langle \Psi_g | S_n^x | \Psi_g \rangle \rightarrow f_0(z) = z + (1/\pi)\sin(\pi z). \tag{2.30}$$

In figure 5(*a*) we compare this result in the one-domain wall approximation with numerical results for the Ising chain in a transverse field (model (iii)). The agreement illustrates that the restriction to the one-domain wall subspace is an excellent approximation for the parameters used. Corresponding results can be given for excited states. For the first excited state the result is given in figure 5(*b*); here the transition from -1 to $+1$ occurs in two steps. For higher excited states this transition takes an increasing number of steps, until a behaviour that is close to linear is obtained in the middle of the band. We then find that these lowest excitations are rather well described by the physical concept of a domain wall moving in a well, and that non-linearity has little effect in this context.

The spatial variation of the transition between the two equivalent groundstates as shown in figure 5 appears qualitatively similar to classical soliton shapes, e.g. to the sine–Gordon soliton. The important difference, however, is that the approach to the asymptotic values is by a power law and not exponential. This observation indicates a

basic difference in the structure of domain walls in $S = \frac{1}{2}$ spin chains as compared with classical chains: in classical chains the domain wall is centred at an arbitrary site and the transition from $-S$ to $+S$ occurs in several steps in a finite region in space. In $S = \frac{1}{2}$ chains the corresponding local transition is from $-\frac{1}{2}$ to $+\frac{1}{2}$ and therefore takes place at a single site, the quantum mechanical possibility of hopping to a neighbouring site then, however, leads to a spreading of this extremely localized structure over the whole chain. A behaviour in direct analogy to the classical one is possible only when the hopping is forbidden by conservation laws. This is the case for model (i) with ferromagnetic coupling, where S^z_{tot} is conserved. In this case even for $S = \frac{1}{2}$ the domain wall remains localized, merely getting dressed by spin waves. The quantum mechanically induced spreading of the domain wall over the whole chain has a direct analogue in a classical model in two dimensions, where it corresponds to the distribution of an interface. We briefly describe this analogy in the appendix.

In our treatment above, all domain walls are centred at the middle of the chain; this is due to the boundary conditions, which require a symmetric behaviour. Although in principle this influence of the boundary conditions is also present in the classical case, there is an important quantitative difference: the energy associated with shifting a localized wall to an arbitrary site on the chain decreases exponentially with N in the classical case, but only as $1/N$ in the quantum case. In this sense, the equivalence of different sites, which classically can be safely assumed in practice, is removed in the quantum system.

Our result is consistent with indications found in the approach of Puga and Beck (1982). These authors have calculated the analogue of the classical soliton contribution to the out-of-plane dynamic structure factor for the $S = \frac{1}{2}$ anisotropic xy model and have found a narrowing of the q dependence. This narrowing reflects the increased spatial extent and should be considered as the experimentally accessible signature of the domain wall structure of Ising-like $S = \frac{1}{2}$ chains as opposed to the corresponding classical systems.

On the other hand, the quantum correction to the spatial width of the classical sine-Gordon soliton as discussed by Mikeska *et al* (1989) in a semiclassical approach is of a different nature: the increase in width with $1/S$ found in this approach is to be understood as a quantum broadening of the classical local spatial structure. This structure will also be subject to quantum diffusion, i.e. to the tendency to spread over the whole chain. However, a theory for finite $S \neq \frac{1}{2}$ is required to describe this fully.

We thus conclude that the one-domain wall approximation is qualitatively, and for small values of h even quantitatively, a good approximation for Ising-like spin chains with $S = \frac{1}{2}$. The most important characteristic of quantum domain walls in chains with this symmetry is that any local spatial structure, which usually characterizes the corresponding classical model, is completely masked by quantum diffusion, which allows the domain wall to spread over the whole chain.

3. Domain wall scattering by impurities

In this section we will study the scattering of a domain wall by impurities in a $S = \frac{1}{2}$ Ising-like magnetic chain. On the one hand this will illustrate the concept of a domain wall as a particle by studying its motion; on the other hand, this problem has attracted interest experimentally in order to understand the result of NMR experiments (Goto 1989, Ferre *et al* 1983), in particular for the effect of domain wall diffusion on T_1 (Boucher *et al* 1985,

Ajiro *et al* 1989). We will consider the Ising model with transverse interactions ((1.1), (1.2)) for antiferromagnetic coupling and will study two different types of impurities:

(i) A quenched magnetic impurity on the chain at site $N+1$. Putting $S^x_{N+1} = +\frac{1}{2}$ we write the Hamiltonian as

$$\mathcal{H} = \mathcal{H}_{\text{Ising}} + \mathcal{H}'_1 + (J + J_e)S^x_N. \tag{3.1}$$

In the special case $J_e = -J$ we obtain the case of a non-magnetic impurity, which, however, is identical to the case of a finite chain treated in the last section.

(ii) Impurities on a neighbouring chain. In this case we introduce an interchain interaction as

$$\mathcal{H}_{\text{interchain}(n,m)} = 2[J'_{yz}(S^y_n S^y_m + S^z_n S^z_m) + J'_x S^x_n S^x_m]$$

where m denotes the position of the neighbour of n on the neighbouring chain. If the lattice is complete, the contributions from two neighbouring chains, with oppositely oriented spins, cancel. An impurity on one neighbouring chain, however, results in a magnetic field acting on the spin on site n according to

$$H_{\text{imp}} = J' S^y_n + J'' S^z_n + 2J_D S^x_n.$$

The factor two for the x-component is put in for later convenience. Here we mainly consider the case $J', J'' \ll 2J_D$, that is

$$H_{\text{imp}} = 2J_D S^x_n. \tag{3.2}$$

In order to confirm the one-domain wall approximation we will also study the low energy spectrum of finite chains (mainly 16 spins) in section 3.2. Furthermore, in section 3.3 we will demonstrate the time evolution of scattering of domain walls

$$|\text{state}(t)\rangle = e^{-i\mathcal{H}t}|\text{state}(0)\rangle$$

to confirm the results with the data obtained in the previous sections.

3.1. One-domain wall approximation

As has generally been shown in section 2, we can express the Hamiltonian in the domain wall operators, (2.11). If we are interested in low temperature properties, we could ignore the multi-domain interaction. Thus we arrive at the one-domain wall approximation, namely

$$\mathcal{H} = J\varepsilon \sum_n (d^+_{n-1} d_{n+1} + \text{HC}) \tag{3.3}$$

which is the same as that which Villain (1985) has introduced to discuss the central peak problem and is similar to the approximation used by Devreux and Boucher (1987). In (3.3), $d^+_n = D_n$ is the domain wall creation operator for antiferromagnetic coupling. Here and in the following, energies are measured with respect to the energy $E_{\text{DW}} = |J|$ of one antiferromagnetic domain wall. Let us denote by $|p\rangle$ the state where the domain

wall is between sites $p-1$ and p. Thus the plane wave describing the domain wall is expressed as

$$|k\rangle = \sum_p (a e^{ikp} + b e^{-ikp}) |p\rangle.$$

In a homogeneous chain, $|k\rangle$ is an eigenvector and the eigenvalue is

$$\lambda_k = E_{DW} + 2J\varepsilon \cos(2k). \tag{3.4}$$

Within this approximation, we can straightforwardly calculate properties of scattering, namely the phase shift or the transmission coefficient, etc. For the cases of (3.1), the interesting property is the phase shift. Let the wave function have the form:

$$|\psi\rangle = \sum_p \psi(p) |p\rangle \tag{3.5}$$

with

$$\psi(p) = e^{ikp} + re^{-ikp} \qquad \text{for} \quad p \leqslant N$$
$$\psi(p) = x \qquad \text{for} \quad p = N+1.$$

If the impurity is on the site $N+1$, the eigenvalue problem for the Hamiltonian (3.1) is given by the following equations:

$$J\varepsilon[(e^{ik(p-2)} + re^{-ik(p-2)}) + (e^{ik(p+2)} + re^{-ik(p+2)})] = \lambda_k(e^{ikp} + re^{-ikp}) \qquad \text{for} \quad p < N-1$$

which gives (3.4) and

$$J\varepsilon[(e^{ik(N-3)} + re^{-ik(N-3)}) + x] = \lambda_k(e^{ik(N-1)} + re^{-ik(N-1)}) \qquad \text{for} \quad p = N-1$$
$$J\varepsilon[(e^{ik(N-1)} + re^{-ik(N-1)})] - J_e x = \lambda_k x \qquad \text{for} \quad p = N+1.$$

This gives

$$r = -e^{2ik(N-1)}(J_e - \varepsilon|J|e^{2ik})/(J_e - \varepsilon|J|e^{-2ik}).$$

The phasefactor $e^{2ik(N+1)}$ can be replaced by 1 after shifting the origin. In the case (3.1) with very large J_e, namely $J_e \gg \varepsilon|J|$, we then have $r = -1$ and the phase shift is π.

For the case of (3.2) we are interested in the transmission phenomena and use the *ansatz* (3.5) for the case of an impurity on the neighbouring chain at site n_{imp} ($N \gg n_{imp} \gg 1$) with

$$\psi(p) = e^{ikp} + re^{-ikp} \qquad \text{for} \quad p < n_{imp}$$
$$\psi(p) = x \qquad \text{for} \quad p = n_{imp}$$
$$\psi(p) = te^{ik'p} \qquad \text{for} \quad p > n_{imp}.$$

Here the eigenvalue problem is given by

$$J\varepsilon[(e^{ik(p-2)} + re^{-ik(p-2)}) + (e^{ik(p+2)} + re^{-ik(p+2)})] + J_D(e^{ikp} + re^{-ikp})$$
$$= \lambda_k(e^{ikp} + re^{-ikp}) \qquad \text{for} \quad p < n_{imp} - 2 \tag{3.6}$$
$$J\varepsilon[(e^{ik(n_{imp}-4)} + re^{-ik(n_{imp}-4)}) + x] + J_D(e^{ik(n_{imp}-2)} + e^{-ik(n_{imp}-2)})$$
$$= \lambda_k(e^{ik(n_{imp}-2)} + e^{-ik(n_{imp}-2)}) \qquad \text{for} \quad p = n_{imp} - 2$$
$$J\varepsilon[(e^{ik(n_{imp}-2)} + re^{-ik(n_{imp}-2)})] + J\varepsilon te^{ik'(n_{imp}+2)} + xJ_D = \lambda_k x \qquad \text{for} \quad p = n_{imp}$$

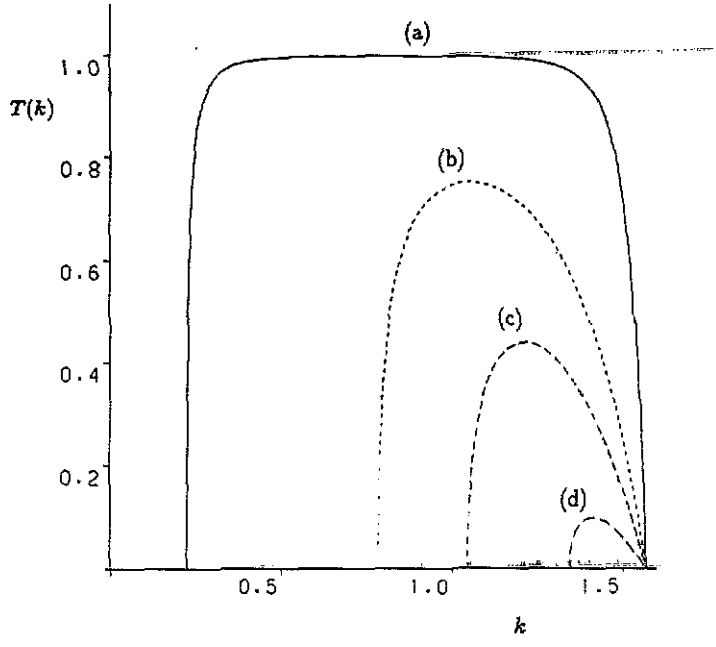

Figure 6. k dependence of the transmission coefficient $T(k)$. $J_D/\varepsilon|J| =$ (*a*) 0.1, (*b*) 1.0, (*c*) 1.5 and (*d*) 1.9.

$$J\varepsilon[x + te^{ik'(n_{\text{imp}}+4)}] - J_D te^{ik'(n_{\text{imp}}+2)} = \lambda_k te^{ik'(n_{\text{imp}}+2)} \qquad \text{for} \quad p = n_{\text{imp}} + 2$$

$$J\varepsilon t[e^{ik'(p-2)} + e^{ik'(p+2)}] - J_D te^{ik'p} = \lambda_k te^{ik'p} \qquad \text{for} \quad p > n_{\text{imp}} + 2. \tag{3.7}$$

From (3.6) and (3.7) we find

$$\lambda_k = J_D + 2\varepsilon|J|\cos(2k) = -J_D + 2\varepsilon|J|\cos(2k')$$

i.e.

$$\cos(2k') = \cos(2k) + J_D/\varepsilon|J|.$$

The remaining equations give the transmission coefficient

$$T(k) = \sin(2k')/\sin(2k)|t|^2 = \sin(2k)\sin(2k')/\sin^2(k + k').$$

Thus $T(k)$ depends only on the ratio $J_D/\varepsilon|J|$. If this ratio is larger than 2.0, no solution for k' exists, which means $T(k) = 0$. In figure 6, the k-dependence of T is plotted for several ratios. For negative values of the ratio, $T(k)$ is obtained by putting $k \to \pi/2 - k$. Here we find that the domain wall cannot pass the impurity from either side, namely from the high energy region to the low energy region or the opposite, if $J_D \gg \varepsilon|J|$. Thus, if we have a strong magnetic field at a site on the chain, the domain wall is reflected by it regardless of the side from which the domain wall incidents. But if we have a strong field at two neighbouring sites domain walls can be transmitted because the wavevectors

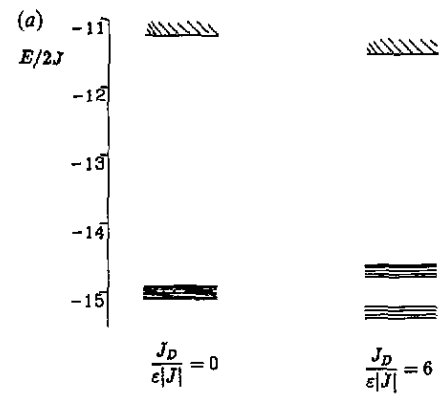

Figure 7. (*a*) The energy spectra for $J_D = 0.0$ and 0.3; the shaded areas denote the band of three-domain wall states. (*b*) Wave functions for $J_D = 0.0$. (*c*) Wave functions for $J_D = 0.3$. Symbols ○, △, +, ×, ⊗, *, ✡, □, X correspond to the ground state and *i*th excited states ($i = 1$ to 8), respectively.

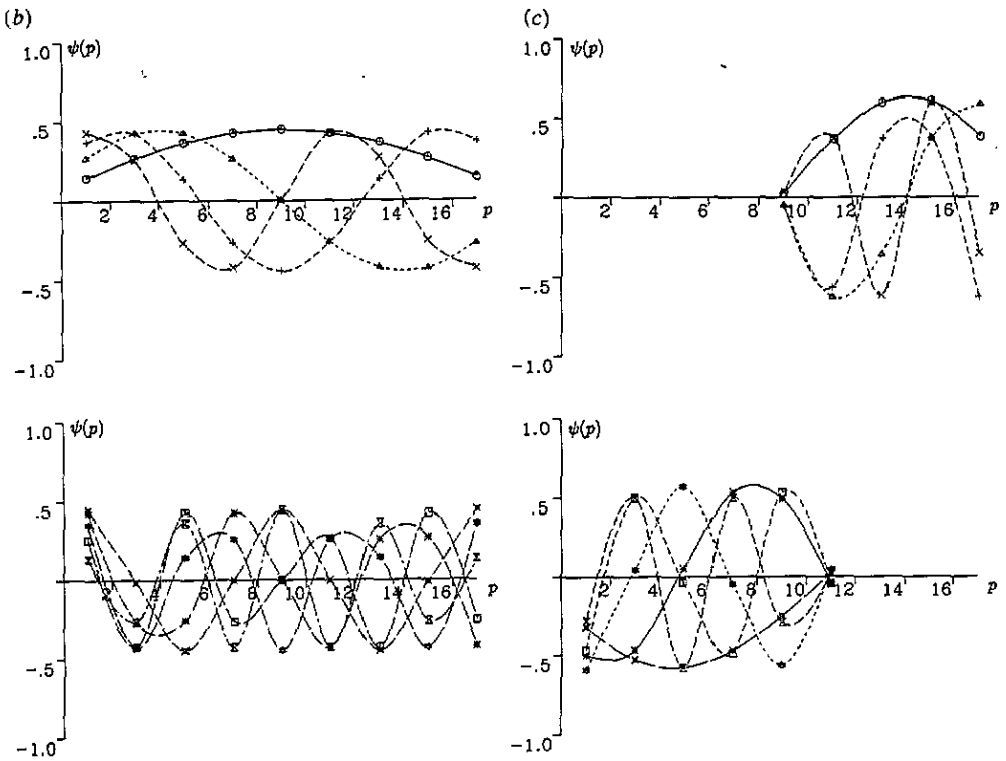

k and k' to the left and to the right of these two sites, respectively, are the same. The transmission coefficient for this case can be calculated similarly to the case treated above.

3.2. Energy spectrum (band structure) of finite lattices

In this section we will study the energy spectrum for finite chains by a direct numerical method and compare them with those expected from the one-domain wall approximation in order to check this approximation. We mainly investigate a chain with 18 spins using boundary conditions which fix the spins at sites $n = 0$ and $n = 17$ as down, thus enforcing an odd number of domain walls for antiferromagnetic coupling. In figure 7(*a*), the

eigenvalues without and with an impurity of type (3.2) at the position $n_{\text{imp}} = 8$ with $J_D = 0.3$ are shown. The value of $\varepsilon|J|$ is 0.05. The eigenfunctions are expressed as

$$|\psi\rangle = \sum_p \psi(p)|p\rangle + \sum_j c_j|j\rangle$$

where $|p\rangle$ is a one-domain wall state as used in the previous section and $|j\rangle$ denotes a multi-domain state.

In figure 7(b), $\psi(p)$ is plotted for the system without impurity and for $J_D = 0$. $\psi(p)$ is the probability amplitude for a domain wall between sites p and $p + 1$ ($p = 0, 1, \ldots 16$). The wavefunctions $\psi(p)$ for the lower four states are given in the upper graph and the others are in the lower. In figure 7(c), the corresponding data for $J_D = 0.3$ are given. It should be noted that the eigenstates in figure 7(b) and those in figure 7(c) are not adiabatically connected.

We find that $\Sigma_j|c_j|^2$ is less than 10^{-2}. We also find that the band of one-domain wall states is well separated from the band of three-domain wall states. In figure 7(a) the shaded area shows the band of three-domain wall states (two-domain wall states cannot appear due to the boundary condition). Furthermore, the shape of the wave function is not much different from that obtained by the approximation. Thus the approximation in the subspace of one-domain wall states is confirmed by the numerical results.

The band structure clearly shows the effect of an impurity of type (3.2): the band of one-domain wall states is well separated into two bands for $J_D/\varepsilon|J| > 2$. Each band consists of states which have a domain wall on one side of the impurity (left or right hand side). Thus no transmission occurs through the impurity. On the other hand if $J_D \leqslant \varepsilon|J|$, then the two bands overlap and we have finite transmission coefficients.

3.3. Initial value problem in finite lattices

In order to visualize what we have discussed in the previous sections, let us perform a real-time development of the wave function:

$$|\psi(t)\rangle = \mathrm{e}^{-\mathrm{i}\mathcal{H}t}|\psi(0)\rangle.$$

In order to perform this time evolution, we used a method based on the Suzuki–Trotter decomposition (Suzuki 1987)

$$\mathrm{e}^{-\mathrm{i}\mathcal{H}\Delta t} \sim \prod_{(ij)} \mathrm{e}^{-\mathrm{i}\mathcal{H}_{ij}\Delta t} \tag{3.8}$$

for small enough Δt and iterated them. We also tested an approximation

$$\mathrm{e}^{-\mathrm{i}\mathcal{H}\Delta t} \sim 1 - \mathrm{i}\left(\sum_{(ij)} \mathcal{H}_{ij}\Delta t\right) - \tfrac{1}{2}\left(\sum_{(ij)} \mathcal{H}_{ij}\Delta t\right)^2.$$

The result is the same within numerical error if we use a small enough value of Δt. The form (3.8), however, strictly conserves the normalization of the wave function because $\mathrm{e}^{-\mathrm{i}\mathcal{H}_{ij}t}$ is a unitary transformation. Thus, we mainly used this approach in the present study.

In a finite lattice, it is difficult to study the transmission coefficient. Thus, we investigated the confinement of a domain wall by the impurities of type (3.2) and the behaviour

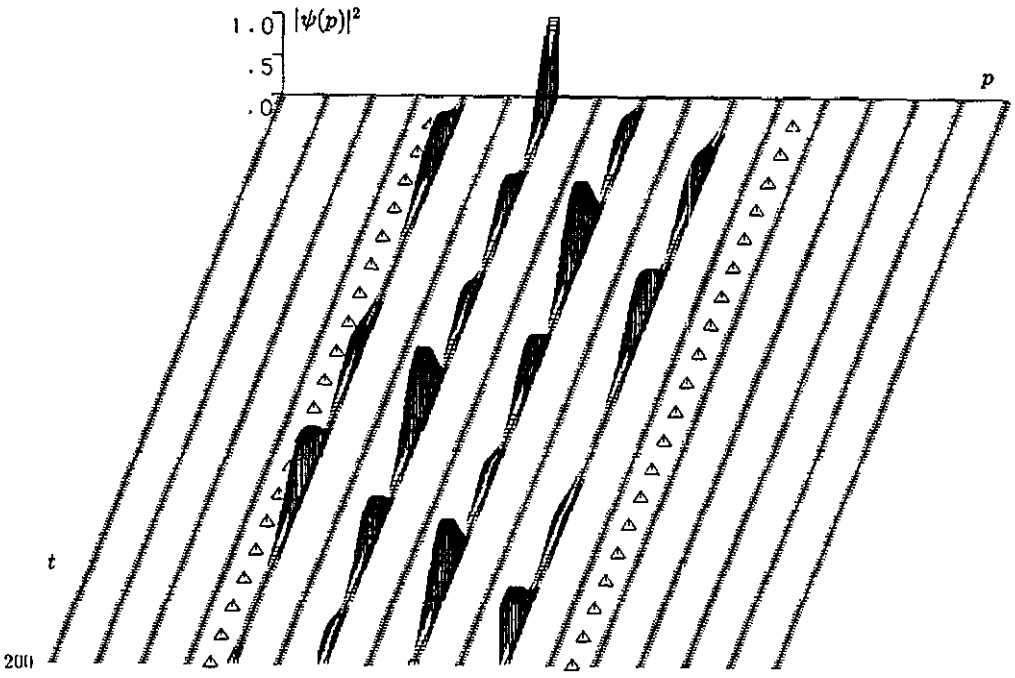

Figure 8. Domain wall confinement. Time dependence of $|\psi(p)|^2$ with an initial configuration $\psi(p) = \delta_{p,6}$.

of a wave packet at the impurity. In figure 8, the confinement of a domain wall between two impurities is demonstrated. As we see here, a domain wall is confined regardless of the relative energy. Here we have the same lattice as used in section 3.2 with impurities of type (3.2) at $n_{\text{imp}} = 4$ and 12 (positions shown by triangles). The values of J_D and $\varepsilon|J|$ are 0.3 and 0.05, respectively. Then the Zeeman energy E_Z due to (3.2) is $-2J_D$ for $l = 1$ and 3, zero for $l = 5, 7, 9$ and 11 and $2J_D$ for $l = 13, 15$ and 17, respectively. Thus the positions 1 and 3 are energetically the most stable ones. But we still find the confinement of a domain wall between the impurities. If we take into account thermal noise, the unstable situation will decay and the domain wall will be released. This finite-temperature effect will be studied in the future.

As we discussed in section 2, it is difficult quantum mechanically to distinguish a domain wall in real space in a good quantum state, since quantum fluctuations cause a diffusion of domain walls. Even so, it would be interesting to see how a wave packet

$$|p_0\rangle = \sum_k e^{-(a/2)(k-k_0)^2}|k\rangle \simeq \sum_k e^{-(a/2)(k-k_0)^2} \sum_p e^{ik(p-p_0)}|p\rangle \tag{3.9}$$

is scattered by impurities. Because we can treat only finite lattices, it is difficult to have a very smooth wave packet. Here we take $a = 4$, $k_0 = 0.3\pi$ and $p_0 = 5$. In figure 9, the propagation of the wavepacket (3.9) is given. Here $\varepsilon|J|$ is 0.05. Because the plane wave has a dispersion relation (3.4), the wavepacket decays after travelling some distance. If

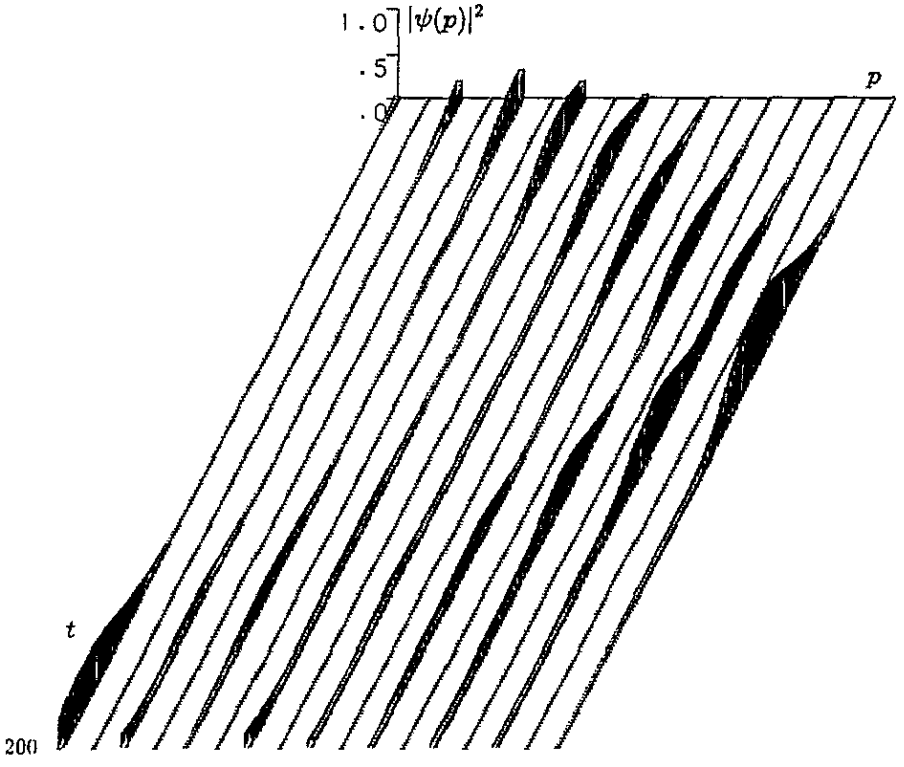

Figure 9. Propagation of a wave packet of domain wall states.

we put an impurity of type (3.2) with $J_D = 0.3$ at some position, the wave packet is reflected in a manner similar to that shown in figure 8.

4. Summary and discussion

In one-dimensional Heisenberg models with Ising-like anisotropy the domain wall is a fundamental excitation, which naturally reminds us of the soliton excitation in the corresponding classical system. In order to study the effect of domain walls, we have introduced a domain wall representation of operators and expressed several models, (1.2–1.4), using this notation. Thus we can define a state $|m\rangle$ with a domain wall at the mth position (2.26), which has a localized shape as shown in figure 2 and should be a counterpart of a classical state with a soliton at the position m.

On the other hand, the domain wall representation naturally leads to the one-domain wall approximation, which has been used intuitively before. The one-domain wall approximation turns out to give the ground state $|\Psi_g\rangle$ for boundary spins fixed opposite to each other to be a state where the system has a very smooth transition between the two degenerate states $|0\downarrow\rangle$ and $|0\uparrow\rangle$ (figure 5). This suggests that quantum fluctuations cause a diffusion of the localized domain wall; a localized shape with a finite width which is determined by the parameters of the Hamiltonian cannot be stable.

In order to check which of the states $|m\rangle$ and $|\Psi_g\rangle$ gives the better approximation to the true ground state, we investigated finite lattices with the boundary conditions mentioned before. The result agrees qualitatively and also quantitatively very well with the result of the one-domain wall approximation. Thus we conclude that in one-dimensional $S = \frac{1}{2}$ chains quantum fluctuations are relevant and smear out the localized domain wall of the corresponding classical system. The effect of quantum fluctuations of the domain wall is also considered in the interface fluctuation in the two-dimensional Ising model with a corresponding boundary condition; this gives a more intuitive understanding of the quantum diffusion.

From an experimental point of view the increased spatial extent owing to quantum diffusion should be related to a narrowing of the structure factors in Ising-like $S = \frac{1}{2}$ chains. Whereas the relevance of domain walls for the interpretation of elastic and inelastic neutron scattering experiments on $CsCoCl_3$ has clearly been demonstrated (Yoshizawa *et al* 1981, Boucher *et al* 1985), a more detailed interpretation of such experiments to show the peculiarities of quantum domain walls requires further theoretical work.

The dynamical nature of the domain wall is also an interesting problem. The one-domain wall approximation allows us to introduce the concept of plane waves of domain walls. We can then study the scattering of domain walls. We have done this in the one-domain wall approximation and confirmed the results on finite chains by direct numerical approaches. As a realistic model for the results presented in section 3 we consider $CsCoCl_3$, where $J = 75\,\mathrm{K}$, $J_D = 0.13\,\mathrm{K}$ and $\varepsilon \sim 0.1$ (Tellenbach and Arend (1977); Yoshizawa *et al* 1981). In this material, impurities in the neighbour chain cause a magnetic field because the interchain interactions cancel each other if the lattice is complete. For $\varepsilon J \gg J_D$ the scattering rate, as given in section 3.1, is very small (see figure 6). If, however, stronger magnetic impurities, leading to $\varepsilon J \ll J_D$, are introduced, the confinement effect discussed in section 3.3 could be observed. In such a case, it would be interesting to study experimentally the temperature dependence of the confinement, which was mentioned in section 3.3. A theoretical study of this problem will be given elsewhere.

Acknowledgments

This work has been supported by the Stiftung Volkswagenwerk and by the German Minister for Research and Technology (BMFT) under contract number 03-MI2HAN-3. The numerical calculations were performed at the Regionales Rechenzentrum für Niedersachsen, Hannover. One of the authors (SM) would like to thank the Institute of Theoretical Physics, University of Hannover, for its stimulative atmosphere and the hospitality. He also thanks Professor T Goto, who kindly informed him about the general experimental situation.

Appendix. Quantum domain walls and the classical interface problem

The problem of diffusion of a domain wall by quantum fluctuation can be related to the interface fluctuations in the two-dimensional Ising model, which can be constructed from the quantum chain (1.4), by the Suzuki–Trotter decomposition (Suzuki 1976,

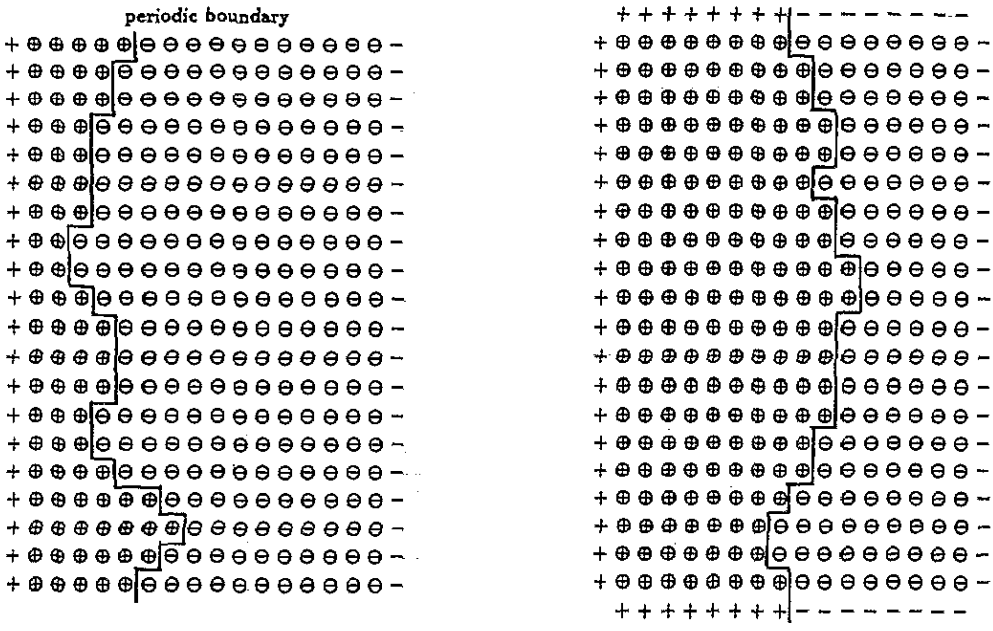

Figure 10. Interface configuration of two-dimensional Ising models (*a*) representing the Hamiltonian $\mathcal{H}_3$, and (*b*) as used for the problem of interface roughening.

1985). Here let us demonstrate this fact for model 3 (1.4) with fixed boundary spins at sites 0 (up) and $N+1$ (down):

$$\begin{aligned}\operatorname{Tr} e^{-\beta\mathcal{H}_3} &= \operatorname{Tr}\exp\left(\beta J\sum_{n=1}^{N-1}\sigma_n^x\sigma_{n+1}^x+\beta J(\sigma_1^x-\sigma_N^x)+\beta H\sum_{n=1}^{N}\sigma_n^z\right)\\ &= \operatorname{Tr}\left[\exp\left(\frac{\beta J}{M}\sum_{n=1}^{N-1}(\sigma_n^x\sigma_{n+1}^x+\sigma_1^x-\sigma_N^x)\right)\prod_{n=1}^{N}e^{(\beta H/M)\sigma_n^z}\right]^M+O\left(\frac{\beta}{M}\right)^2 \qquad (A.1)\\ &= Z_{(M)}+O\left(\frac{\beta}{m}\right)^2.\end{aligned}$$

Following the well known procedure as described by Suzuki (1976) we have

$$\begin{aligned}Z_{(M)} = \operatorname{Tr} A^{MN}\exp\Bigg[&(\beta J/M)\left(\sum_{n=1}^{N-1}\sum_{m=1}^{M}\sigma_n^{(m)}\sigma_{n+1}^{(m)}+\sigma_1^{(m)}-\sigma_N^{(m)}\right)\\ &+K'(M)\sum_{n=1}^{N-1}\sum_{m=1}^{M}\sigma_n^{(m)}\sigma_n^{(m+1)}\Bigg] \qquad (A.2)\end{aligned}$$

where $\sigma_i^{(m)}=\sigma_i^{(m+M)}=\pm 1$, $A^2=\cosh(\beta H/M)\sinh(\beta H/M)$, $e^{-2K'(M)}=\tanh(\beta H/M)$. $Z_{(M)}$ is the partition function of an anisotropic Ising model on a $N\times M$ two-dimensional lattice with boundary conditions as shown in figure 10(*a*). In this notation, the spin

density $\langle \sigma_n^x \rangle$ is expressed by $\langle \sigma_n^{(m)} \rangle$ for any value of m. This problem is quite similar to the interface problem which has been studied with the boundary condition shown in figure 10(b) (Binder 1983, Abraham 1981, Bricmont *et al* 1981). There, the shape of $\langle \sigma_n^{(m)} \rangle$ has been obtained to have a Gaussian profile with the interface width of the order of $\sqrt{N}$.

In the present model, (A.2), the length M and the coupling constants are not independent, moreover the boundary condition in the M-direction is periodic and does not specify the position of the domain wall. Thus we cannot make use of the results of the conventional interface problem directly. Instead we will give a rough estimate in the following.

Since we want to study the ground state of the original quantum model, we put $\beta \to \infty$. We assume ($K_0 = \beta J/M$)

$$\sinh(2K'(M)) \sinh(2K_0) > 1 \qquad \text{namely } H < J \tag{A.3}$$

which assures the ordering of the ground state and also guarantees that the 2D lattice is at $T < T_c$. $\langle \sigma_n^{(m)} \rangle$ can be obtained by considering the behaviour of the domain walls on the lattice of figure 10(a). Roughly speaking the probability of side steps of the domain wall p is

$$p = \tanh(\beta H/M)/[1 + \tanh(\beta H/M)]. \tag{A.4}$$

Because the lattice has length M, the width of the domain wall is of the order of

$$\Delta \simeq \sqrt{M} p. \tag{A.5}$$

In particular in the limit $\beta/M \to 0$, which makes the correction in (A.1) negligible, we have

$$\Delta \simeq \sqrt{M}(\beta H/M) \sim \beta H/\sqrt{M}. \tag{A.6}$$

To discuss the limit $\beta/M \to 0$, we have to consider two physically different situations: if we take $M > \beta \gtrsim \sqrt{M}$, Δ diverges when $\beta \to \infty$. Since we have boundaries at $n = 0$ and $n = N + 1$, $\Delta = \infty$ in this situation means that M is sufficiently long for the domain wall to make a random walk, forgetting the position at $m = 1$. It will therefore behave as a free particle in a well. If we take $M \gg \beta^2$, then we have $\Delta \sim 0$. But in this case we can shift the position of the domain wall parallel to the M direction because we have not fixed the boundary condition (in contrast to the situation studied for the roughening transition, figure 10(b)). A free particle-like behaviour again results from this global shifting of the domain wall.

Thus we conclude that in either case, when the correction $O(\beta/M)^2 \to 0$, the distribution of the domain wall position is that of a free particle in a well and thus determined by the probability distribution leading to (2.30). The diffusive property of the domain walls in the $S = \frac{1}{2}$ chain is seen to be closely analogous to the interface fluctuations in the corresponding 2D Ising model. This analogy has already emerged in the present rough treatment of the interface distribution. A rigorous treatment, which includes the effects from multi-domain states, similar to the one given by Bricmont *et al* (1981), requires further work.

References

Abraham D B 1981 *Phys. Rev. Lett.* **47** 545

Ajiro Y, Kikuchi H, Okita T, Chiba M, Adachi K, Mekata M and Goto T 1989 *J. Phys. Soc. Japan* **58** 390
Binder K 1983 *Phase Transitions and Critical Phenomena* vol 8, ed C Domb and J L Lebowitz (New York: Academic) p 2
Boucher J P, Regnault L P, Rossat-Mignod J, Henry Y, Bouillot J and Stirling W G 1985 *Phys. Rev.* B **31** 3015
Bricmont J, Lebowitz J L and Pfister C E 1981 *J. Stat. Phys.* **26** 313
Buyers W J L 1983 *The Neutron and its Applications* (Bristol: Institute of Physics)
Devreux F and Boucher J P 1987 *J. Physique* **48** 1663
Elstner N and Mikeska H J 1989 *J. Phys.: Condens. Matter* **1** 1487
Ferre J, Renard J P and Briat B 1983 *J. Phys. C: Solid State Phys.* **16** 1099
Goto T 1989 private communication
Ishimura N and Shiba H 1980 *Prog. Theor. Phys.* **63** 743
Kjems J K and Steiner M 1978 *Phys. Rev. Lett.* **41** 1137
Lieb E, Schultz T and Mattis D 1961 *Ann. Phys., NY* **16** 407
Mikeska H J 1978 *J. Phys. C: Solid State Phys.* **11** L29
Mikeska H J 1981 *J. Appl. Phys.* **52** 1950
Mikeska H J, da Costa B V and Fogedby H C 1989 *Z. Phys.* B **77** 119
Mikeska H J and Miyashita S 1990 unpublished
Mikeska H J and Steiner M 1990 *Adv. Phys.* at press
Pesch W and Mikeska H J 1978 *Z. Phys.* B **30** 177
Pfeuty P 1970 *Ann. Phys., NY* **57** 79
Prelovšek P and Sega I 1981 *Phys. Lett.* **81A** 407
Puga M W and Beck H 1982 *J. Phys. C: Solid State Phys.* **15** 2441
Regnault L P, Boucher J P, Rossat-Mignot J, Renard J P, Bouillot J and Stirling W G 1983 *J. Phys. C: Solid State Phys.* **15** 1261
Smit H H A, de Groot H J M, Elmassalami M, Thiel R C and de Jongh L J 1989 *Physica* B **154** 237
Steiner M and Bishop A R 1986 *Solitons* ed S E Trullinger, V E Zakharov and V L Pokrovsky (Amsterdam: North-Holland)
Steiner M, Kakurai K and Kjems J K 1983 *Z. Phys.* B **53** 117
Suzuki M 1976 *Prog. Theor. Phys.* **56** 1454
Suzuki M 1985 *Phys. Lett.* **113A** 299
Suzuki M (ed) 1987 *Monte Carlo Method of Equilibrium and Non-equilibrium Systems* (Berlin: Springer)
Tellenbach U and Arend H 1977 *J. Phys. C: Solid State Phys.* **10** 1311
Villain J 1975 *Physica* B **79** 1
Yoshizawa H, Hirakawa K, Satija S K and Shirane G 1981 *Phys. Rev.* B **23** 2298